



Explaining the thickness-dependent dielectric permittivity of thin films

Alessio Zaccone *

Department of Physics “A. Pontremoli”, University of Milan, via Celoria 16, 20133 Milan, Italy
and Institute for Theoretical Physics, University of Göttingen, Friedrich-Hund-Platz 1, 37077 Göttingen, Germany

 (Received 14 November 2023; revised 13 March 2024; accepted 14 March 2024; published 28 March 2024)

The dielectric properties of thin films are of paramount importance in a variety of technological applications, and of fundamental importance for solid-state research. In spite of this, there is currently no theoretical understanding of the dependence of the dielectric permittivity on the thickness of thin films. We develop a confinement model within the Lorentz-field framework for the microscopic Langevin-equation description of dielectric response in terms of the atomic-scale vibrational modes of the solid. Based on this, we derive analytical expressions for the dielectric permittivity as a function of thin-film thickness, in excellent agreement with the experimental data of barium-strontium-titanate thin films of different stoichiometry. The theory shows that the decrease of dielectric permittivity with decreasing thickness is directly caused by the restriction in k space of the available eigenmodes for the field-induced alignment of ions and charged groups.

DOI: [10.1103/PhysRevB.109.115435](https://doi.org/10.1103/PhysRevB.109.115435)

I. INTRODUCTION

The physical properties of thin films are crucial for a variety of technological applications, ranging from optical mirrors to solar cells [1,2], and of fundamental interest in physics. In particular, understanding the dielectric properties of solid thin films is vital in optics, e.g., dielectric (Bragg) mirrors, thin-film interference (antireflective coatings), optical and protective coatings, microwave devices, memory devices, and 5G wireless communication. Dielectric and electrical properties may strongly depend on thin-film thickness, which is a problem of both fundamental and technological interest [3–5]. In particular, size effects give rise to changes in the electrical performance of thin-film capacitors and field-effect transistors, including issues such as depolarization fields in the dielectric sandwiched between semiconductors [6], and polarization screening in metal-dielectric-metal thin-film capacitors [7]. Finally, thin films are known to have enhanced or ultrahigh dielectric strength, which is another important thickness-dependent effect [8]. In spite of these tremendous technological implications, there currently exists no quantitative theoretical description of the dependence of dielectric properties on film thickness. This is also due to the intrinsic limitations of *ab initio* methods which cannot simulate thicknesses of more than a few nanometers [9,10]. Here we provide a microscopic theory able to quantitatively describe this effect.

II. THEORY

A. Langevin equation framework for lattice ions

We describe the dynamics of charged groups (ions), and of partially charged groups, in a solid material by means of a generalized Langevin equation (GLE) [11,12]. Since we

are interested in determining the dielectric response of the material, we have to use a GLE that contains the appropriate Lorentz force term due to the external oscillating electric field, and which contains a stochastic force term that obeys a suitable fluctuation-dissipation theorem. Denoting the mass-rescaled tagged-particle displacement $s = Q\sqrt{M}$, where M is the mass of the ion (or of the partially charged group) and Q is the displacement vector, the resulting equation of motion reads as [12]

$$\ddot{s} = -U'(s) - \int_0^t \nu(t-t') \frac{ds}{dt'} dt' + F(t) + zE(t), \quad (1)$$

where $U(s)$ denotes the local force field, and ν is the microscopic friction due to the long-range nonlocal anharmonic interactions with the thermal bath represented by all other atoms and ions present in the system. Furthermore, $F(t)$ is the stochastic force representing the thermal noise, and the last term on the right-hand side is the Lorentz force term relating to the system’s response to the external AC electric field, where the charge z has been redefined to be the mass-scaled charge. In order to determine the dependence of the polarization and of the dielectric function on the frequency of the field in three-dimensional (3D) space, we have to describe the displacement \mathbf{s} of each charged particle from its own equilibrium position under the applied AC field $\mathbf{E}(t)$. Upon treating the dynamics classically, the equation of motion for a charge I under forces coming from interactions with other atoms in the system and from the applied AC electric field is given by

$$\ddot{s}_I^\mu = - \sum_{j\nu} H_{IJ}^{\mu\nu} s_j^\nu - \int_0^t \nu(t-t') \frac{ds_I^\mu}{dt'} dt' + F_I^\mu(t) + z_I E^\mu(t), \quad (2)$$

under the assumption of pairwise interactions, and the Greek index μ denotes the space components of a vector.

*alessio.zaccone@unimi.it

The next step is to take the Fourier transform, $s_I^\mu(t) \rightarrow \tilde{s}_I^\mu(\omega)$, leading to

$$-\omega^2 \tilde{s}_I^\mu(\omega) + i\omega \tilde{v}(\omega) \tilde{s}_I^\mu(\omega) + H_{IJ}^{\mu\nu} \tilde{s}_J^\mu(\omega) = \tilde{F}_I^\mu + z_I \tilde{E}^\mu, \quad (3)$$

where the tilde is used to indicate Fourier-transformed quantities. Hence, $\tilde{v}(\omega)$ denotes the Fourier transform of $v(t)$. Since the Hessian matrix $H_{IJ}^{\mu\nu}$ is real and symmetric and its eigenvectors provide a basis set in Hilbert space, we can apply normal-mode decomposition by projecting the $3N$ -dimensional Fourier-transformed displacement vector \tilde{s} onto the $3N$ -dimensional eigenvectors of the Hessian: $\hat{s}_m(\omega) = \tilde{s}(\omega) \cdot e_m$. Here the hat is used to denote the coefficient of the projected quantity, e_m represent orthonormal eigenvectors of the Hessian matrix, and m runs from 1 to $3N$. Then we obtain

$$-\omega^2 \hat{s}_m + i\omega \tilde{v}(\omega) \hat{s}_m + \omega_m^2 \hat{s}_m = \hat{F}_m + (z\hat{E})_m. \quad (4)$$

The equation is solved by

$$\hat{s}_m(\omega) = -\frac{\hat{F}_m + (z\hat{E})_m}{\omega^2 - i\omega \tilde{v}(\omega) - \omega_m^2}. \quad (5)$$

Upon transforming back to a vector equation for the Fourier-transformed displacement of charge I , we have

$$\sum_I \tilde{s}_I(\omega) = \sum_m -\frac{\tilde{\mathbf{F}} + z\tilde{\mathbf{E}}}{\omega^2 - i\omega \tilde{v}(\omega) - \omega_m^2}, \quad (6)$$

where $\tilde{\mathbf{F}}$ and $\tilde{\mathbf{E}}$ are average values.

B. Polarization and dielectric function

Each charged particle contributes a moment $\mathbf{p}_I = z_I \mathbf{s}_I$ to the moment. In order to evaluate the macroscopic polarization, we add together the averaged contributions from all microscopic degrees of freedom in the system, $\mathbf{P} = \sum_I \mathbf{p}_I$. In order to do this analytically, we use the fact that the ensemble average of the noise for an oscillating system vanishes upon averaging over many cycles, as also demonstrated numerically in Ref. [13]. We thus employ the sum over all contributions of the type given by Eq. (6) to obtain the averaged polarization. We also perform the standard procedure of replacing the discrete sum over the total degrees of freedom of the solid with the continuous integral over the eigenfrequencies $\omega_m, \sum_m \dots \rightarrow \int g(\omega_p) \dots d\omega_p$, where $g(\omega_p)$ is the vibrational density of states (VDOS). This gives the following sum rule for the electric polarization [14]:

$$\tilde{\mathbf{P}}(\omega) \propto -\left[\int_0^{\omega_D} \frac{g(\omega_p)}{\omega^2 - i\omega \tilde{v}(\omega) - \omega_p^2} d\omega_p \right] \tilde{\mathbf{E}}(\omega). \quad (7)$$

Here, ω_D is the cutoff Debye frequency arising from the normalization of the VDOS (i.e., the highest eigenfrequency in the vibrational spectrum). Furthermore, we have defined a $3N$ -dimensional vector \vec{z} such that $\hat{z}_m = \vec{z} \cdot e_m$ is a scalar factor, arising from Eq. (6) [15], which is later going to be absorbed into the prefactor A and therefore is no longer shown in the above relation.

Note that we have taken an ensemble average over the system. The complex dielectric permittivity ϵ is defined as $\epsilon = 1 + 4\pi \chi_e$, where χ_e is the dielectric susceptibility, which relates the polarization and electric field via $\mathbf{P} = \chi_e \mathbf{E}$ [16].

Within this model [14], the dielectric function is finally expressed as a frequency integral as [14]

$$\epsilon(\omega) = 1 - A \int_0^{\omega_D} \frac{g(\omega_p)}{\omega^2 - i\omega \tilde{v}(\omega) - \omega_p^2} d\omega_p, \quad (8)$$

where A is an arbitrary positive constant whose numerical value has to be matched with experiments. Clearly, if $g(\omega_p)$ were given by a Dirac δ , one would recover the standard simple-exponential Debye relaxation [14,17]. This approach can be extended to deal with atoms and molecules that have stronger inner polarizability by replacing the external field \mathbf{E} with the local electric field \mathbf{E}_{loc} , which is known as the Lorentz cavity model or Lorentz field [17,18]. In condensed matter, the net electric field that acts on a molecule locally is equal to the external field only for vanishing polarizability of the molecule. This is a well-known effect, whereby the field in the medium is influenced (typically, diminished) by the local alignment of the nearby polarized molecules. The simple Lorentz cavity model works well in materials where the building blocks are not pathologically shaped or too anisotropic. In order to keep the treatment analytical, we focus on the case of constant friction, $v = \text{const}$. The derivation of the local field or Lorentz field can be found in many textbooks [17,18] and gives

$$\mathbf{E}_{\text{loc}} = \mathbf{E} + \frac{4\pi}{3} \mathbf{P}. \quad (9)$$

Therefore, \mathbf{E} is replaced with the Lorentz field \mathbf{E}_{loc} , and the equation of motion becomes

$$\tilde{s}'_I(\omega) = \frac{z_I}{\omega^2 - i\omega v - \omega_p^2} \left[\tilde{\mathbf{E}}(\omega) + \frac{4\pi}{3} \tilde{\mathbf{P}}(\omega) \right]. \quad (10)$$

Combining the above relations and summing over all contributions from all the ions and charged groups, we obtain

$$\mathbf{P} = \left(\sum_I q_I \mathbf{s}_I + \alpha \mathbf{E}_{\text{loc}} \right), \quad \epsilon(\omega) = 1 + 4\pi \frac{\chi(\omega)}{1 - \frac{4\pi}{3} \chi(\omega)},$$

$$\chi(\omega) = \int_0^{\omega_D} \frac{A g(\omega_p)}{\omega^2 - \omega_p^2 + i\omega v} d\omega_p + \alpha, \quad (11)$$

where α is the microscopic electronic polarizability and we used the definition of electric displacement vector $\mathbf{D} = \epsilon \mathbf{E} = \mathbf{E} + 4\pi \mathbf{P}$ [19]. Furthermore, in the expression of χ , we have incorporated the factor z^2 into the rescaling coefficient A . This microscopic theory of the dielectric response has been previously applied to describe experimental data of supercooled glycerol in Ref. [14] and was able to explain the non-Debye asymmetric excess wing of the dielectric loss $\epsilon''(\omega)$ as due to the excess of low-energy vibrational modes that characterize the vibrational spectra of supercooled liquids and glasses.

C. Thin-film confinement and thickness-dependent permittivity

The above form of the dielectric function is derived for a bulk material. In the case of a thin film, the confinement along the vertical direction imposes a constraint on the wavelength of the vibrational excitations that are allowed to propagate [20]. As shown mathematically in Ref. [21], and verified against MD simulations and experiments for real thin solid films in [22], the thin-film confinement imposes a

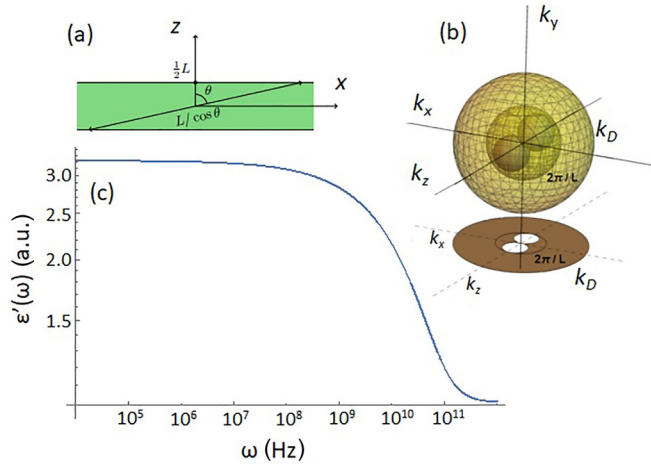


FIG. 1. (a) The thin-film geometry in real space (confined along the z axis but unconfined along the x and y axes), with the maximum wavelength that corresponds to a certain polar angle θ . (b) The corresponding geometry of k space, where the outer Debye sphere (of radius k_D) contains two symmetric spheres of forbidden states, i.e., states in k space that remain unoccupied due to confinement along the z axis. See Ref. [21] for a detailed mathematical derivation of this result. (c) An illustrative calculation of the dielectric permittivity using the confined model, with typical values of speed of sound (of the order of kHz and of microscopic friction ν and Debye frequency both of the order of 10^{13} Hz. (a) and (b) have been adapted from Ref. [21] with permission.

low-frequency cutoff on the wave vector of vibrational modes equal to $k_{\min} = \frac{2\pi \cos \theta}{L}$. Here, L is the film thickness and θ is the polar angle with the vertical z axis; see Fig. 1. The condition $k_{\min} = \frac{2\pi \cos \theta}{L}$ identifies two spheres of forbidden states inside the Debye sphere.

As demonstrated in Ref. [22], this lower cutoff wave vector corresponds to a minimum frequency of the allowed vibrational modes given by $\omega_{\min} = c k_{\min}$, where c is a characteristic speed of sound (independent of L). For example, c can be taken as the average speed of sound c used in Debye's theory, defined as $\frac{3}{c^3} = \frac{1}{c_L^3} + \frac{2}{c_T^3}$, where c_L and c_T are the longitudinal and the transverse speed of sound, respectively. Since the minimum wave vector depends on the polar angle θ , we can take a spherical average over the solid angle that gives the average minimum wave vector $\bar{k}_{\min} = \frac{\pi}{L}$, and a minimum frequency $\bar{\omega}_{\min} = \frac{c\pi}{L}$. Upon implementing this confinement-induced cutoff in the susceptibility integral, we get

$$\epsilon(\omega) = 1 + 4\pi \frac{\chi(\omega)}{1 - \frac{4\pi}{3} \chi(\omega)},$$

$$\chi(\omega) = \alpha + \int_{\frac{c\pi}{L}}^{\omega_D} \frac{A g(\omega_p)}{\omega^2 - \omega_p^2 + i\omega\nu} d\omega_p. \quad (12)$$

As a sanity check, we plot in Fig. 1(c) a typical behavior of the dielectric permittivity $\epsilon'(\omega)$ computed using Eq. (12) for realistic values of frequencies encountered in solid materials. The resulting curve still presents all the typical features of dielectric permittivity as a function of frequency, with a low-frequency plateau followed by a drop (dielectric relaxation)

in the frequency range 10^8 – 10^9 Hz typically measured in dielectric spectroscopy [23].

In order to understand the effect of film thickness L on the permittivity ϵ' , the integral in Eq. (12) has to be evaluated. Using a Debye law for the vibrational density of states, $g(\omega_p) \sim \omega_p^2$, as appropriate for a solid, the integral cannot be evaluated analytically. Nevertheless, we can approximate the integral for low-to-intermediate frequencies ω since this is the regime of interest for measurements of dielectric permittivity of thin solid films. Using the approximation $\omega_p \gg \omega$, for the real part of the integral, we obtain

$$\int \frac{\omega_p^4}{\omega_p^4 + \omega^2 \nu^2} d\omega_p \approx \omega_p - \sqrt{\frac{\nu \omega}{2}} \arctan \left(\frac{\sqrt{2} \omega_p}{\sqrt{\nu \omega}} \right). \quad (13)$$

With the integration limits set in Eq. (12) and neglecting nonlinear contributions to the susceptibility, this leads to the following expression for the thickness-dependent dielectric permittivity:

$$\epsilon'(\omega) = \epsilon_\infty + A \frac{4\pi(\omega_D - \frac{c\pi}{L}) + \sqrt{\frac{\nu \omega}{2}} \arctan \left(\frac{\sqrt{2} \omega_p}{\sqrt{\nu \omega}} \frac{c\pi}{L} \right) - B}{1 - \frac{4\pi}{3} A \omega_D + \frac{4\pi}{3} A \frac{c\pi}{L}},$$

$$B = A \sqrt{\frac{\nu \omega}{2}} \arctan \left(\frac{\sqrt{2} \omega_D}{\sqrt{\nu \omega}} \right). \quad (14)$$

We note that in the limit $L \rightarrow \infty$, the above expression correctly tends to a constant value independent of L , which represents the bulk value at a given frequency ω . The above expression (14) can be Taylor expanded in L to study the leading terms that control the thickness-dependent dielectric permittivity of thin films. To second order in L , we thus obtain

$$\epsilon'(\omega) = \epsilon_\infty + K_1 L - K_2 L^2 + O(L^3), \quad (15)$$

where

$$K_1 = \frac{9 - 3B}{A'}, \quad K_2 \approx \frac{4\pi A^2 \sqrt{\nu \omega} \omega_D}{A'^2}, \quad (16)$$

and where $A' \equiv 4\pi^2 A c$ has units of an inverse length, which is reassuring because then, in Eq. (15), all terms are dimensionless, as they should be.

III. COMPARISON WITH EXPERIMENTAL DATA

For thin-film oxides at low to intermediate frequencies, $\omega = 1$ – 10 kHz, one has $\epsilon' \sim 10$ – 100 from experimental measurements. Then it is clear that the rescaling constant A , which, in the above, multiplies the Debye frequency $\omega_D \sim 10^{13}$ Hz, must be of the order of $A \sim 10^{-12}$, and hence, in general, a small number. From the first one of Eqs. (16), it follows that $K_1 > 0$ always, provided that $\frac{9}{A} > \frac{3B}{A} = 3\sqrt{\nu \omega}$. This is always true because, for realistic values of experimental systems, one has $\sqrt{\nu \omega} \sim 10^8$ – 10^9 Hz, which is orders of magnitude smaller than $\frac{3}{A} \sim 10^{12}$ Hz. We thus conclude that K_1 is always positive and therefore the leading term in the expansion is such that the dielectric permittivity increases with increasing L . This means that, overall, the confinement acts as to lower the dielectric permittivity. The above microscopic theory explains that physically, this is due to the cutting off of low-frequency vibration eigenmodes at the atomic level due

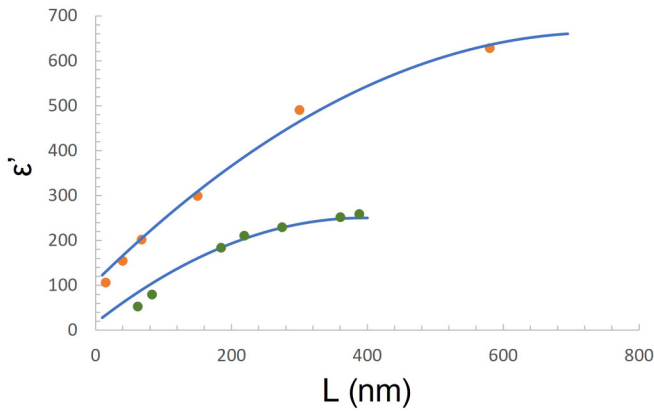


FIG. 2. Comparison between the theoretical prediction given by Eq. (15), continuous line, and experimental data (circles). The latter are in arbitrary physical units, as customary for dielectric spectroscopy measurements. The upper curve refers to experimental data of the dielectric permittivity of $(\text{Ba}_{0.7}, \text{Sr}_{0.3})\text{TiO}_3$ (BST) thin films measured at $\omega = 4$ kHz from Ref. [3], fitted by Eq. (15) with $K_1 = 1.5$ and $K_2 = 0.001$, and $\epsilon_\infty = 100$. The lower curve refers to experimental data of the dielectric permittivity of $(\text{Ba}_{0.5}, \text{Sr}_{0.5})\text{TiO}_3$ thin films averaged between $\omega = 400$ Hz and $\omega = 10$ kHz from Ref. [24], fitted by Eq. (15) with $K_1 = 1.2$ and $K_2 = 0.0015$, and $\epsilon_\infty = 10$. All experimental measures were made at room temperature.

to the confinement, which, in turn, leads to more limited possibilities for the ions and charged groups to spatially rearrange (“align”) in response to the local electric field.

The second term in the expansion is, instead, negative and acts as to level off the initial increase as a function of thickness L . Furthermore, with realistic values of the physical parameters as declared above, we have that $K_2 \sim 10^7$ since $\sqrt{\nu\omega} \sim 10^8$ Hz and $c \sim 10^4$ m/s, while $K_1 \sim 10^{10}$ and thus $K_2/K_1 \sim 0.001$.

This observation then leaves just one nontrivial fitting parameter in the comparison between Eq. (15) and the experimental data, which is reported in Fig. 2. The nontrivial fitting parameter is ϵ_∞ , which represents the infinite-frequency limit of the dielectric permittivity and is thus controlled by the atomic-scale physics.

Furthermore, the value of ϵ_∞ is also constrained to be reasonable and much smaller than the bulk value at kHz

frequencies, which is indeed the case in the fitting shown in Fig. 2. This further consideration reflects the fact that the above fitting is physically meaningful and reliable.

IV. CONCLUSION

In summary, we have developed a microscopic theory of dielectric response of thin solid films starting from a Langevin equation for the motion of charged and partially charged atoms in the solid layer. Using a recent wave-confinement model, we have adapted the theory to the case of thin films, by implementing a cutoff in momentum space reflecting the fact that a significant population of large-wavelength vibrational modes becomes forbidden due to the thin-film confinement. In turn, this reduces the possibilities for atomic-scale rearrangements/alignments under the applied field, leading to a lower permittivity for thinner films. The theory leads to an analytical expression for the dielectric permittivity as a function of applied field frequency and film thickness, in excellent agreement with experimental data with just one nontrivial fitting parameter (ϵ_∞), which, however, is constrained to be in a reasonable range by the material physics. In future work, this theory can be extended to nanoconfined liquid films, including nanoconfined water [25,26]. To this aim, it may be useful to also provide a formulation of the above theory for off-diagonal tensor components [27]. It can also be extended to ultrathin films (with thickness of the order of few nanometers or lower), where the vibrational density of states features a low-energy ω^3 behavior, instead of Debye’s ω^2 law [22]. In the future, this theory can open up different ways to tune and optimize the electrical performance of thin-film devices, ranging from photovoltaics to 5G technology, and to understand and model the ultrahigh dielectric strength of thin films [8].

ACKNOWLEDGMENTS

The author gratefully acknowledges funding from the European Union through Horizon Europe ERC Grant No. 101043968 “Multimech,” from the U.S. Army Research Office through Contract No. W911NF-22-2-0256, and from the Niedersächsische Akademie der Wissenschaften zu Göttingen in the frame of the Gauss Professorship program. Discussion and input from S. Achilli and G. Onida are gratefully acknowledged.

-
- [1] A. Shah, P. Torres, R. Tscherner, N. Wyrsh, and H. Keppner, Photovoltaic technology: The case for thin-film solar cells, *Science* **285**, 692 (1999).
 - [2] J. M. Ball, S. D. Stranks, M. T. Hörantner, S. Hüttner, W. Zhang, E. J. W. Crossland, I. Ramirez, M. Riede, M. B. Johnston, R. H. Friend, and H. J. Snaith, Optical properties and limiting photocurrent of thin-film perovskite solar cells, *Energy Environ. Sci.* **8**, 602 (2015).
 - [3] C. B. Parker, J.-P. Maria, and A. I. Kingon, Temperature and thickness dependent permittivity of $(\text{Ba},\text{Sr})\text{TiO}_3$ thin films, *Appl. Phys. Lett.* **81**, 340 (2002).
 - [4] K. Natori, D. Otani, and N. Sano, Thickness dependence of the effective dielectric constant in a thin film capacitor, *Appl. Phys. Lett.* **73**, 632 (1998).
 - [5] I. A. Starkov and A. S. Starkov, The thickness dependence of dielectric permittivity in thin films, *J. Phys.: Conf. Ser.* **741**, 012004 (2016).
 - [6] I. P. Batra, P. Wurfel, and B. D. Silverman, Phase transition, stability, and depolarization field in ferroelectric thin films, *Phys. Rev. B* **8**, 3257 (1973).
 - [7] C. T. Black and J. J. Welsler, Electric-field penetration into metals: Consequences for high-dielectric-constant capacitors, *IEEE Trans. Electron Devices* **46**, 776 (1999).
 - [8] J. Liu, J. Su, L. Zhao, R. Li, Y. Lu, and X. Liu, Influence of dielectric constant on dielectric strength by defect discharge and molecular polarization in solid insulation materials, *J. Appl. Phys.* **125**, 115103 (2019).

- [9] K. Yim, Y. Yong, J. Lee, K. Lee, H.-H. Nahm, J. Yoo, C. Lee, C. Seong Hwang, and S. Han, Novel high- κ dielectrics for next-generation electronic devices screened by automated *ab initio* calculations, *NPG Asia Mater.* **7**, e190 (2015).
- [10] M. Stengel and N. A. Spaldin, Origin of the dielectric dead layer in nanoscale capacitors, *Nature (London)* **443**, 679 (2006).
- [11] W. T. Coffey and Y. P. Kalmykov, *The Langevin Equation*, 3rd ed. (World Scientific, Singapore, 2012).
- [12] B. Cui and A. Zaccone, Generalized Langevin equation and fluctuation-dissipation theorem for particle-bath systems in external oscillating fields, *Phys. Rev. E* **97**, 060102(R) (2018).
- [13] T. Damart, A. Tanguy, and D. Rodney, Theory of harmonic dissipation in disordered solids, *Phys. Rev. B* **95**, 054203 (2017).
- [14] B. Cui, R. Milkus, and A. Zaccone, Direct link between boson-peak modes and dielectric α -relaxation in glasses, *Phys. Rev. E* **95**, 022603 (2017).
- [15] B. Cui, Microscopic theory of linear response in amorphous materials, Ph.D. thesis, Apollo - University of Cambridge Repository, 2020.
- [16] M. Born and E. Wolf, *Principles of Optics* (Cambridge University Press, Cambridge, 1999).
- [17] H. Froehlich, *Theory of Dielectrics* (Clarendon Press, Oxford, 1958).
- [18] T. C. Choy, *Effective Medium Theory* (Oxford University Press, Oxford, 2015).
- [19] J. Jackson, *Classical Electrodynamics*, 3rd ed. (Wiley, Hoboken, NJ, 1998).
- [20] A. Zaccone and K. Trachenko, Explaining the low-frequency shear elasticity of confined liquids, *Proc. Natl. Acad. Sci. USA* **117**, 19653 (2020).
- [21] A. E. Phillips, M. Baggioli, T. W. Sirk, K. Trachenko, and A. Zaccone, Universal L^{-3} finite-size effects in the viscoelasticity of amorphous systems, *Phys. Rev. Mater.* **5**, 035602 (2021).
- [22] Y. Yu, C. Yang, M. Baggioli, A. E. Phillips, A. Zaccone, L. Zhang, R. Kajimoto, M. Nakamura, D. Yu, and L. Hong, The ω^3 scaling of the vibrational density of states in quasi-2D nanoconfined solids, *Nat. Commun.* **13**, 3649 (2022).
- [23] F. Kremer and A. Schoenhals, *Broadband Dielectric Spectroscopy* (Springer, Berlin, 2003).
- [24] J. Oh, T. Moon, T.-G. Kim, C. Kim, J. H. Lee, S. Y. Lee, and B. Park, The dependence of dielectric properties on the thickness of (Ba,Sr)TiO₃ thin films, *Curr. Appl. Phys.* **7**, 168 (2007).
- [25] E. Papadopoulou, J. Zavadlav, R. Podgornik, M. Praprotnik, and P. Koumoutsakos, Tuning the dielectric response of water in nanoconfinement through surface wettability, *ACS Nano* **15**, 20311 (2021).
- [26] H. Yang, G. Ji, M. Choi, S. Park, H. An, H.-T. Lee, J. Jeong, Y. D. Park, K. Kim, N. Park, J. Jeong, D.-S. Kim, and H.-R. Park, Suppressed terahertz dynamics of water confined in nanometer gaps, [arXiv:2310.19236](https://arxiv.org/abs/2310.19236).
- [27] C. A. Valagiannopoulos, On measuring the permittivity tensor of an anisotropic material from the transmission coefficients, *Prog. Electromagn. Res. B* **9**, 105 (2008).